DOI:10.1111/j.1365-2125.2005.02472.x

Physiologically based pharmacokinetic modelling of the three-step metabolism of pyrimidine using ^{13}C-uracil as an *in vivo* probe

Suminobu Ito, Takeshi Kawamura,[1] Makoto Inada,[2] Yoshiharu Inoue,[3] Yukihiro Hirao,[4] Toshihisa Koga,[4] Jun-ichi Kunizaki,[2] Takefumi Shimizu[2] & Hitoshi Sato[5]

Department of Clinical Pharmacology, Juntendo University School of Medicine, Tokyo, [1]Department of Nursing, Miyagi University, Miyagi [2]Research Section, Diagnostics Division and [3]Formulation Research Institute, Otsuka Pharmaceutical Co., Ltd, Tokushima, [4]Department of Drug Metabolism, Drug Safety Research Centre, Tokushima Research Institute, Otsuka Pharmaceutical Co., Ltd, Tokushima, and [5]Department of Clinical and Molecular Pharmacokinetics/Pharmacodynamics, School of Pharmaceutical Sciences, Showa University, Tokyo, Japan

Correspondence
Makoto Inada, Otsuka Pharmaceutical Co., Ltd, 224–18 Ebisuno, Hiraishi, Kawauchi-cho, Tokushima 771–0182, Japan.
Tel.: +81 88 665 8988
Fax: +81 88 665 8344
E-mail: inadam@otsuka.jp

Keywords
^{13}C-, dihydropyrimidine dehydrogenase (DPD), physiologically based pharmacokinetic (PBPK) model, uracil

Received
21 December 2004
Accepted
25 May 2005

Aims
Approximately 80% of uracil is excreted as β-alanine, ammonia and CO_2 via three sequential reactions. The activity of the first enzyme in this scheme, dihydropyrimidine dehydrogenase (DPD), is reported to be the key determinant of the cytotoxicity and side-effects of 5-fluorouracil. The aim of the present study was to re-evaluate the pharmacokinetics of uracil and its metabolites using a sensitive assay and based on a newly developed, physiologically based pharmacokinetic (PBPK) model.

Methods
[2–^{13}C]Uracil was orally administrated to 12 healthy males at escalating doses of 50, 100 and 200 mg, and the concentrations of [2–^{13}C]uracil, [2–^{13}C]5,6-dihydrouracil and β-ureidopropionic acid (ureido-^{13}C) in plasma and urine and $^{13}CO_2$ in breath were measured by liquid chromatography–tandem mass spectrometry and gas chromatograph–isotope ratio mass spectrometry, respectively.

Results
The pharmacokinetics of [2–^{13}C]uracil were nonlinear. The elimination half-life of [2–^{13}C]5,6-dihydrouracil was 0.9–1.4 h, whereas that of [2–^{13}C]uracil was 0.2–0.3 h. The AUC of [2–^{13}C]5,6-dihydrouracil was 1.9–3.1 times greater than that of [2–^{13}C]uracil, whereas that of ureido-^{13}C was 0.13–0.23 times smaller. The pharamacokinetics of $^{13}CO_2$ in expired air were linear and the recovery of $^{13}CO_2$ was approximately 80% of the dose. The renal clearance of [2–^{13}C]uracil was negligible.

Conclusion
A PBPK model to describe $^{13}CO_2$ exhalation after orally administered [2–^{13}C]uracil was successfully developed. Using [2–^{13}C]uracil as a probe, this model could be useful in identifying DPD-deficient patients at risk of 5-fuorouracil toxicity.

Introduction

Pyrimidine and purine, which are present endogenously in nucleic acids, nucleotides and their derivatives, display a wide range of physiological functions. Since the catabolism and anabolism of pyrimidines are inextricably linked, their biological fate is complex. Uracil, a pyrimidine base, is metabolized to β-alanine, ammonia and CO_2 via three sequential reactions [1, 2] (Figure 1).

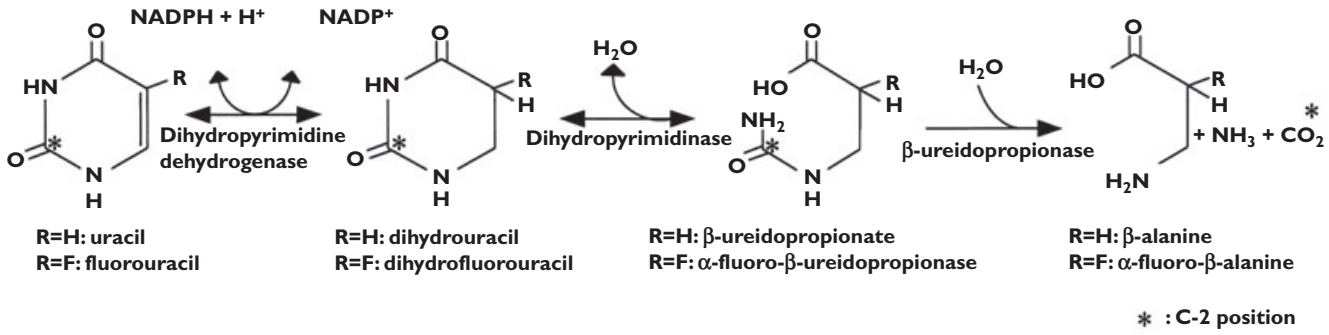

Figure 1
The metabolism of uracil and 5-fluorouracil in humans

Uracil is first reduced to dihydrouracil by dihydropyrimidine dehydrogenase (DPD), then hydrolysed to β-ureidopropionic acid by dihydropyrimidinase (DHPase), and finally decarbamoylated to β-alanine by β-ureidopropionase (UP). Of these enzymes, DPD is considered to represent the rate-limiting step [3, 4].

5-Fluorouracil (5-FU) is an anticancer agent in which the hydrogen atom at the C-5 position of uracil is substituted by fluorine (Figure 1). Since the structure of 5-FU is analogous to that of uracil, it is biotransformed to putative, biologically active metabolites, 5-fluoro-2′-deoxyuridine-5′-monophosphate or 5-fluorouridine-5′-triphosphate, by the same anabolic pathway as that of uracil [5, 6]. 5-FU is metabolized by conversion to biologically inactive metabolites by the same enzymes that metabolize uracil [7–10]. When 5-FU is given to patients with genetic DPD deficiency or those taking drugs which inhibit DPD activity, blood concentrations of the drug are markedly elevated, resulting in serious adverse effects [11–14]. The use of diagnostic methods to detect pyrimidine metabolic disorders [15–17] at the start of chemotherapeutic treatment would prevent the development of adverse effects with 5-FU and its prodrugs.

We previously developed a diagnostic product (UBIT®) for *Helicobacter pylori* infection which measures *in vivo* urease activity using expired $^{13}CO_2$ after oral administration of ^{13}C-urea [18–20]. Extending this work, we have developed a new method for diagnosing pyrimidine metabolic disorders using [2–^{13}C]uracil (^{13}C-uracil), prepared by labelling the C-2 position of uracil with ^{13}C, a stable isotope of ^{12}C (Figure 1). We have already applied this method to dogs [21] to show that expired $^{13}CO_2$ is a good marker of hepatic DPD activity in the enzyme-deficient model. To gain further understanding of pyrimidine catabolism, the pharmacokinetics of ^{13}C-uracil was studied following oral administration under fasting conditions to healthy subjects at escalating doses.

Methods

Subjects

The study protocol was approved by the Ethics Committee of Juntendo University Hospital, and written informed consent was obtained from each participant before enrolment. The subjects were 12 healthy Japanese males (21–57 years old; 56–90 kg) with normal pyrimidine metabolism as determined by measurement [22] of endogenous pyrimidine and dihydropirimidine in urine. Good general health was confirmed by 12-lead electrocardiogram, medical history and physical examination. The study was designed to evaluate the pharmacokinetic profile of ^{13}C-uracil and its metabolites after single oral administration of ^{13}C-uracil using an open label, single-centre, dose escalation design. The subjects were given ^{13}C-uracil on three occasions at escalating doses of 50, 100 and 200 mg under fasted conditions. The subjects were given ^{13}C-uracil as granules with 100 ml of water at approximately 09.00 h. Food was not permitted from 21.00 h on the evening before dosing to 4 h after dosing. Subjects were in a sitting position for 2 h postdose. The order of dosing was 50, 100 and 200 mg and the wash-out period was set at ≥5 days. Blood was taken immediately before and at 10, 20, 30, 40, 50, 60 and 90 min and 2, 4, 6, 8 and 12 h after dosing. Urine samples were collected before and at the periods of 0–2, 2–4, 4–8 and 8–12 h after dosing. Breath samples were collected in a bag (volume 300 ml) before and at 10, 20, 30, 40, 50, 60, 80 and 100 min and 2, 3, 4, 6, 8 and 12 h after dosing.

Chemicals

[2-^{13}C]Uracil, [2-^{13}C]5,6-dihydrouracil, β-ureidopropionic acid (ureido-^{13}C), uracil ($^{13}C_4$, $^{15}N_2$), 5,6-dihydrou-

racil ($^{13}C_4$, $^{15}N_2$) and β-ureidopropionic acid ($^{13}C_4$, $^{15}N_2$) were purchased from Cambridge Isotope Laboratories, Inc. (Andover, MA, USA). All other solvents and reagents were of the highest grade available.

Determination of ^{13}C-uracil, ^{13}C-DHU and ^{13}C-UPA in plasma and urine by LC-MS/MS

Plasma concentrations of ^{13}C-uracil and its metabolites (^{13}C-DHU and ^{13}C-UPA) were measured by LC-MS/MS (TSQ7000; Thermo Finnigan, San Jose, CA, USA). Isotope-labelled uracil ($^{13}C_4$, $^{15}N_2$), 5,6-dihydrouracil ($^{13}C_4$, $^{15}N_2$) and β-ureidopropionic acid ($^{13}C_4$, $^{15}N_2$) were used as internal standards. ^{13}C-Uracil and ^{13}C-DHU were extracted from 0.5 ml of plasma using 4 ml of acetonitrile after the addition of 0.5 ml of a saturated aqueous ammonium sulphate solution. Samples were then centrifuged at 2200 *g* for 10 min. The organic layer was evaporated to dryness, the residue reconstituted in 200 µl of purified water, and a 50-µl aliquot was injected into LC-MS/MS. A Develosil RPAQUEAUS column (5 µm, 2.0 mm i.d. ×150 mm; Nomura Chemical Co., Ltd, Seto, Japan) and a mobile phase of water were used to separate the analytes. ^{13}C-UPA was extracted from 0.2 ml of plasma by solid-phase extraction on silica after deproteinization. After evaporation of the eluate to dryness, the residue was reconstituted in 200 µl of purified water. This solution (30 µl) was injected onto the LC-MS/MS fitted with two columns in series, a Develosil RPAQUEAUS (5 µm, 2.0 mm i.d. ×150 mm) and a Capcell pak SCX UG80 (5 µm, 2.0 mm i.d. ×50 mm; Shiseido Co., Ltd, Tokyo, Japan). The mobile phase was an aqueous solution of 10 mM ammonium formate (pH 3.5). Protonated molecular ions $[M+1]^+$ of the analytes including the internal standard, formed by atmospheric pressure chemical ionization, were fragmented, and the selected product ions were monitored (selected reaction monitoring). The calibration curves were linear over the ranges 5–250 ng ml^{-1} for ^{13}C-uracil and ^{13}C-DHU and 50–2000 ng ml^{-1} for ^{13}C-UPA. The percent recoveries of isotope-labelled uracil ($^{13}C_4$, $^{15}N_2$), 5,6-dihydrouracil ($^{13}C_4$, $^{15}N_2$) and β-ureidopropionic acid ($^{13}C_4$, $^{15}N_2$) from human plasma were 83–105%, 56–74% and 23–24%, respectively. The limit of quantification (LOQ), defined as the lowest concentration with a coefficient of variation (CV) of <20% and accuracy within ±20%, was 5 ng ml^{-1} for ^{13}C-uracil and ^{13}C-DHU and 50 ng ml^{-1} for ^{13}C-UPA. Precision, estimated as CV, was <15% and accuracy was within ±15% for the analytes at all concentrations except the LOQ.

Urinary concentrations of each compound were measured using LC-MS/MS. ^{13}C-Uracil and ^{13}C-DHU were extracted from 0.2 ml of urine using 5 ml of ethyl acetate after the addition of 0.1 ml of a saturated aqueous ammonium sulphate solution. The samples were then centrifuged at 1800 *g* for 10 min. After the organic layer was evaporated to dryness, the residue was reconstituted in 200 µl of purified water and 30 µl of the solution was injected onto the LC-MS/MS. ^{13}C-UPA was extracted from 0.1 ml of the urine by solid-phase extraction on silica after deproteinization. After evaporation of the solid-phase extraction eluate to dryness, the residue was reconstituted in 200 µl of purified water and 30 µl was injected onto the LC-MS/MS. The chromatographic conditions were similar to those for the plasma samples. The calibration curves for these analytes were linear over the range of 0.1–5 µg ml^{-1}, and the LOQ was 0.1 µg ml^{-1}. The percent recoveries of isotope-labelled uracil ($^{13}C_4$, $^{15}N_2$), 5,6-dihydrouracil ($^{13}C_4$, $^{15}N_2$) and β-ureidopropionic acid ($^{13}C_4$, $^{15}N_2$) from human urine were 57–64%, 63–74% and 20–30%, respectively. Precision was <15% and accuracy was within ±15% at all concentrations except the LOQ.

Analysis of $^{13}CO_2$ in expired air by gas chromatography isotope ratio mass spectrometry (IRMS)

$^{13}CO_2$ concentrations in expired air were determined using a gas chromatograph-IRMS (model ABCA-G; PDZ-Europa Ltd, Cheshire, UK). $^{13}CO_2/^{12}CO_2$ ratios were expressed as δ^{13}C value (permil, ‰) relative to the Pee Dee Belemnite Limestone standard, and changes in the δ^{13}C value as Δ^{13}C (‰) were compared with the baseline using the following equations:

$$\delta^{13}C\ (‰) = [(^{13}CO_2/^{12}CO_2)_{sample} - (^{13}CO_2/^{12}CO_2)_{PDB}]/(^{13}CO_2/^{12}CO_2)_{PDB} \times 1000$$

$$\Delta^{13}C_t\ (‰) = \delta^{13}C_t - \delta^{13}C_0$$

where $\Delta^{13}C_t$ (‰) is the difference between respiratory $\delta^{13}C_t$ measured at time t and baseline $\delta^{13}C_0$ following the administration of ^{13}C-uracil.

Pharmacokinetic analysis

Pharmacokinetic parameters for ^{13}C-uracil and its metabolites were calculated using noncompartmental pharmacokinetic analysis (WinNonlin Standard version 3.1; Pharsight Co., Mountain View, CA, USA). Maximum plasma concentration (C_{max}), time to C_{max} (t_{max}) and the area under the plasma concentration *vs.* time curve up to 12 h after administration ($AUC_{12\,h}$) were determined. The apparent terminal-phase slope (λ_z) was estimated by linear regression of the semilogarithmic curve of plasma concentration *vs.* time. The terminal elimination half-life ($t_{1/2}$) was calculated as $0.693/\lambda_z$. AUC_∞ was calculated by dividing the last measured concentration (C_{last}) by λ_z. The apparent total clearance (CL/F) is dose/

AUC_∞, and the apparent volume of distribution (V_d/F) is CL/F/λ_z. The cumulative amount excreted into the urine for 12 h (*Ae*) was used to estimate the renal clearance (CL_R) from the expression $Ae/AUC_{12\,h}$. The total amount of $^{13}CO_2$ recovered in the breath (m) was calculated from $^{13}CO_2$ excretion curves based on the method of Ghoos *et al.* [23], in which CO_2 production was assumed to be 300 mmol m^{-2} h^{-1}.

Statistical analysis

The relationships between the dose and the pharmacokinetic parameters (C_{max}, AUC_t, and AUC_∞) were analysed by using a predictive power model based on the equation

$$\text{Parameter} = A\cdot(\text{Dose})^{\beta}$$

Statistical analysis was performed with SAS software, version 8.2 (SAS Institute Japan, Tokyo, Japan).

Model development

A physiologically based pharmacokinetic (PBPK) model model (Figure 2) was constructed to describe the time course of plasma concentrations of ^{13}C-uracil and its metabolites, and $^{13}CO_2$ in expired air. This model incorporates Michaelis–Menten catabolic and first-order degradation processes. The differential equations for the PBPK model were as follows:

For ^{13}C-uracil

$$V_p\cdot(dC_p/dt) = Q_H\cdot C_h/K_p - Q_H\cdot C_p - C_p\cdot CL_R \quad (1)$$

$$V_h\cdot(dC_h/dt) = k_a\cdot F_a\cdot \text{Dose}\cdot e^{-k_a t} - f_p\cdot C_h\cdot CL_{int}/K_p - Q_H\cdot C_h/K_p + Q_H\cdot C_p \quad (2)$$

$$CL_{int} = V_{max}/(K_m + f_p\cdot C_h/K_p) \quad (3)$$

For ^{13}C-DHU

$$V_{dDHU}\cdot(dC_{DHU}/dt) = f_p\cdot C_h/K_p\cdot CL_{int} - C_{DHU}\cdot V_{dDHU}\cdot k_{eDHU} \quad (4)$$

For ^{13}C-UPA

$$V_{dUPA}\cdot(dC_{UPA}/dt) = C_{DHU}\cdot V_{dDHU}\cdot k_{eDHU} - C_{UPA}\cdot V_{dUPA}\cdot k_{eUPA} \quad (5)$$

For $^{13}CO_2$

$$dX_H{}^{13}CO_3^-/dt = C_{UPA}\cdot V_{dUPA}\cdot k_{eUPA} - k_e\cdot X_H{}^{13}CO_3^- \quad (6)$$

$$\Delta^{13}C(‰) = P1 + P2\cdot X_H{}^{13}CO_3^- \quad (7)$$

where V_h is the volume of the liver; V_p is the volume of distribution in rapidly equilibrating tissues, including the systemic plasma compartment of ^{13}C-uracil; V_{dDHU} and V_{dUPA} are the pseudo-distribution volumes of ^{13}C-DHU and ^{13}C-UPA, respectively; C_h is the concentration of ^{13}C-uracil in liver; C_p, C_{DHU} and C_{UPA} are the plasma concentrations of ^{13}C-uracil, ^{13}C-DHU and ^{13}C-UPA, respectively; Q_H is the hepatic blood flow rate; K_p is the liver-to-blood concentration ratio of ^{13}C-uracil; CL_R is the renal clearance of ^{13}C-uracil; CL_{int} is intrinsic metabolic clearance; V_{max} and K_m are the maximum rate of ^{13}C-uracil metabolism and the Michaelis–Menten constant, respectively; f_p is the unbound fraction of ^{13}C-uracil in plasma; k_{eDHU} and k_{eUPA} are the degradation rate constants of ^{13}C-DHU and ^{13}C-UPA, respectively; $X_H{}^{13}CO_3^-$ is the amount of $H^{13}CO_3^-$; k_e is the excretion rate constant of $^{13}CO_2$; and P1 and P2 are constants.

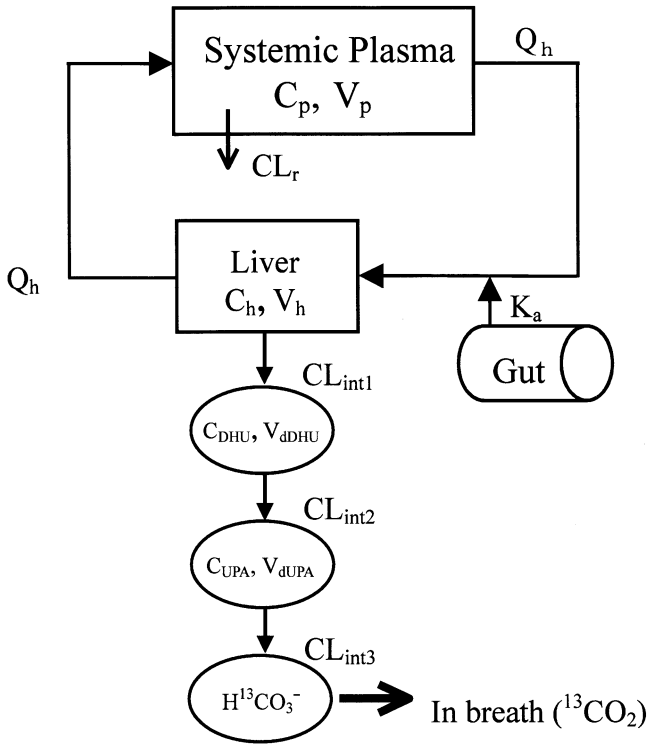

Figure 2
A physiologically based pharmacokinetic model describing the concentration–time profiles for ^{13}C-uracil, its metabolites and $^{13}CO_2$ in expired air

These equations are based on the following assumptions:

1 The gastrointestinal absorption of ^{13}C-uracil follows a first-order process.
2 ^{13}C-Uracil is eliminated by the liver and kidney, and is converted sequentially in the liver to ^{13}C-DHU, ^{13}C-UPA and $H^{13}CO_3^-$.
3 ^{13}C-uracil is eliminated via a single irreversible and saturable Michaelis–Menten process.
4 The elimination of the metabolites of ^{13}C-uracil follows first-order irreversible kinetics.
5 The elimination of ^{13}C-DHU, ^{13}C-UPA and $H^{13}CO_3^-$ is described by a single-compartment model.

This assumption can be justified from the following findings: (i) a single-compartment model describes the pharmacokinetics of $^{13}CO_2$-$H^{13}CO_3^-$ after co-administration of sodium bicarbonate [24]; (ii) the kinetics of $^{13}CO_2$ after administration of ^{13}C-compounds are best described by a one-compartment model [25–27].

Equation 7 holds true because $\Delta^{13}C$ (‰) is proportional to the amount of $H^{13}CO_3^-$ in the body [28]. The physiological data used, namely $V_h = 1070$ ml, $Q_H = 1190$ ml min^{-1} and haematocrit value = 0.55, were obtained from the literature. K_p, f_p and F_a were set at 1.0 according to our preliminary experiments (data not shown), and CL_R at 120 ml min^{-1} on the basis of our urinary excretion analysis.

The pharmacokinetic software SAAM II (SAAM Institute Inc., Seattle, WA, USA) was used for nonlinear least squares analysis to fit the parameters V_p, k_e, K_m and V_{max} to the set of plasma concentrations of ^{13}C-uracil for dose-escalation experiments using equations 1, 2 and 3. Using these fixed parameters, the parameters V_{dDHU}, V_{dUPA}, k_{eDHU}, k_{eUPA}, k_e, P1 and P2 were subsequently estimated by SAAM II using equations 4–7.

Results

Pharmacokinetics

Tables 1, 2 and 3 show the pharmacokinetic parameters for ^{13}C-uracil, ^{13}C-DHU and ^{13}C-UPA in the plasma, respectively, and Tables 4 and 5 the urinary excretion and expiratory $^{13}CO_2$ excretion data. Figure 3 shows the concentration *vs.* time curves for ^{13}C-uracil and its metabolites, and the $\Delta^{13}C$ in the expired air *vs.* time curve.

^{13}C-Uracil was absorbed rapidly after oral dosing to attain C_{max} within 0.54 h, and then declined rapidly in plasma, with a short half-life of less than 0.32 h. The major metabolite of ^{13}C-uracil in plasma at all doses was

Table 1
Pharmacokinetic parameters for ^{13}C-uracil in plasma

Dose	C_{max} (μg ml^{-1})	$AUC_{12\,h}$ (μg h ml^{-1})	AUC_∞ (μg h ml^{-1})	t_{max} (h)	λ_z (1 h^{-1})	$t_{1/2}$ (h)	CL/F (l h^{-1})	V_d/F (l)
50 mg	0.127	0.047	0.053	0.36	3.66	0.26	1082	466
	±0.083	±0.022	±0.021	±0.10	±1.71	±0.22	±410	±500
100 mg	0.534	0.165	0.170	0.39	5.25	0.21	772	296
	±0.430	±0.109	±0.107	±0.18	±2.92	±0.19	±368	±423
200 mg	1.205	0.545	0.567	0.54	2.91	0.32	464	296
	±0.899	±0.325	±0.312	±0.25	±1.19	±0.26	±265	±480

Values: mean ± SD (n = 12).

Table 2
Pharmacokinetic parameters for ^{13}C-DHU in plasma

Dose	C_{max} (μg ml^{-1})	$AUC_{12\,h}$ (μg h ml^{-1})	t_{max} (h)	λ_z (1 h^{-1})	$t_{1/2}$ (h)
50 mg	0.102	0.144	0.49	0.68	1.10
	±0.050	±0.048	±0.15	±0.18	±0.34
100 mg	0.251	0.378	0.56	0.78	0.91
	±0.094	±0.135	±0.18	±0.11	±0.14
200 mg	0.551	1.054	0.93	0.60	1.37
	±0.255	±0.449	±0.50	±0.19	±0.74

Values: mean ± SD (n = 12).

Table 3
Pharmacokinetic parameters for ^{13}C-UPA in plasma

Dose	C_{max} (μg ml^{-1})	$AUC_{12\,h}$ (μg h ml^{-1})	t_{max} (h)	λ_z (1 h^{-1})	$t_{1/2}$ (h)
50 mg	0.023	0.006	0.46	–	–
	±0.035	±0.014	±0.16	–	–
100 mg	0.076	0.034	0.50	1.17	0.87
	±0.040	±0.042	±0.19	±0.88	±0.61
200 mg	0.149	0.126	0.82	1.12	1.05
	±0.081	±0.105	±0.45	±0.67	±1.05

–, Not calculated. Values: mean ± SD (n = 12).

Table 4
Urinary excretion and kinetic parameters for ^{13}C-uracil and its metabolites

Substance	Parameter	50 mg	100 mg	200 mg
^{13}C-uracil	*Ae* (mg)	0.35 ± 0.19	1.21 ± 0.80	4.52 ± 2.80
	CL_R (l h^{-1})	6.8 ± 1.6	7.2 ± 2.1	7.7 ± 1.4
	Excretion (%/dose)	0.7 ± 0.4	1.2 ± 0.8	2.3 ± 1.4
^{13}C-DHU	*Ae* (mg)	0.10 ± 0.05	0.28 ± 0.14	0.83 ± 0.44
	CL_R (l h^{-1})	0.7 ± 0.2	0.7 ± 0.2	0.8 ± 0.3
	Excretion (%/dose)	0.2 ± 0.1	0.3 ± 0.1	0.4 ± 0.2
^{13}C-UPA	*Ae* (mg)	0.21 ± 0.10	0.53 ± 0.31	1.33 ± 0.91
	CL_R (l h^{-1})	17.1 ± 8.7	13.4 ± 6.3	9.1 ± 4.1
	Excretion (%/dose)	0.4 ± 0.2	0.5 ± 0.3	0.6 ± 0.4

^{13}C-DHU: 5,6-dihydrouracil (2-^{13}C)] ^{13}C-UPA, β-ureidopropionic acid (ureido-^{13}C). Values: mean ± SD (n = 12).

Table 5
Expiratory excretion parameters for $^{13}CO_2$ ($\Delta^{13}C$)

Dose	C_{max} (‰)	$AUC_{12\,h}$ (‰ h)	AUC_∞ (‰ h)	t_{max} (h)	λ_z (1 h^{-1})	$t_{1/2}$ (h)	m (% dose^{-1})
50 mg	37.8	53.3	54.2	0.43	0.59	1.27	75.5
	±11.7	±5.3	±5.2	±0.15	±0.18	±0.36	±7.4
100 mg	67.9	106.4	107.8	0.54	0.56	1.41	75.9
	±17.3	±9.7	±9.9	±0.19	±0.21	±0.59	±3.3
200 mg	104.8	213.8	216.2	0.89	0.55	1.34	76.4
	±20.8	±25.0	±24.9	±0.44	±0.15	±0.37	±6.1

m, Amount of $^{13}CO_2$ recovered in the breath. Values: mean ± SD (n = 12).

^{13}C-DHU, with the relative ratios of the $AUC_{12\,h}$ of ^{13}C-DHU to ^{13}C-uracil at 50, 100 and 200 mg being 3.1, 2.3 and 1.9, respectively. ^{13}C-UPA was a minor metabolite, and the relative ratios of the $AUC_{12\,h}$ of ^{13}C-UPA to ^{13}C-uracil at 50, 100 and 200 mg were 0.13, 0.21 and 0.23, respectively. Plasma concentrations of ^{13}C-DHU were higher than those of ^{13}C-uracil from 50 min after administration. At all doses, the elimination half-life of ^{13}C-DHU was much longer than that of ^{13}C-uracil. A predictive power model was used to evaluate the dose-proportionality of C_{max}, $AUC_{12\,h}$ and AUC_∞ values. None of these parameters was dose-proportional over the range of 50–200 mg [the 95% confidence interval (CI) for the slope of the regression line (β) did not include unity]. Nonlinearity in pharmacokinetics was clearly present in 10 out of the 12 subjects, although there was considerable interindividual variability between subjects.

The contribution of renal clearance to the total body clearance was negligible (Table 4).

The $\Delta^{13}C$ of $^{13}CO_2$ in expired air *vs.* time curve was similar to that of ^{13}C-DHU in plasma (Figure 3). The recovery of ^{13}C in expired air was approximately 80% at each dose, which is in agreement with previous reports [8–10] on the deposition of 5-FU. C_{max} was found not to be dose-proportional over the range of 50–200 mg, but AUC_∞ and $AUC_{12\,h}$ were proportional to dose [the 95% CIs of the slopes (β) for these parameters were 0.93–1.06 and 0.94–1.06].

The predicted concentration–time courses of ^{13}C-uracil, ^{13}C-DHU, ^{13}C-UPA and $\Delta^{13}C$ (‰) are shown in Figure 4. Satisfactory agreement between the predicted curve and experimental data was obtained. The exception was the relationship for ^{13}C-UPA, which had a higher limit of quantification (50 ng ml^{-1}) than with ^{13}C-

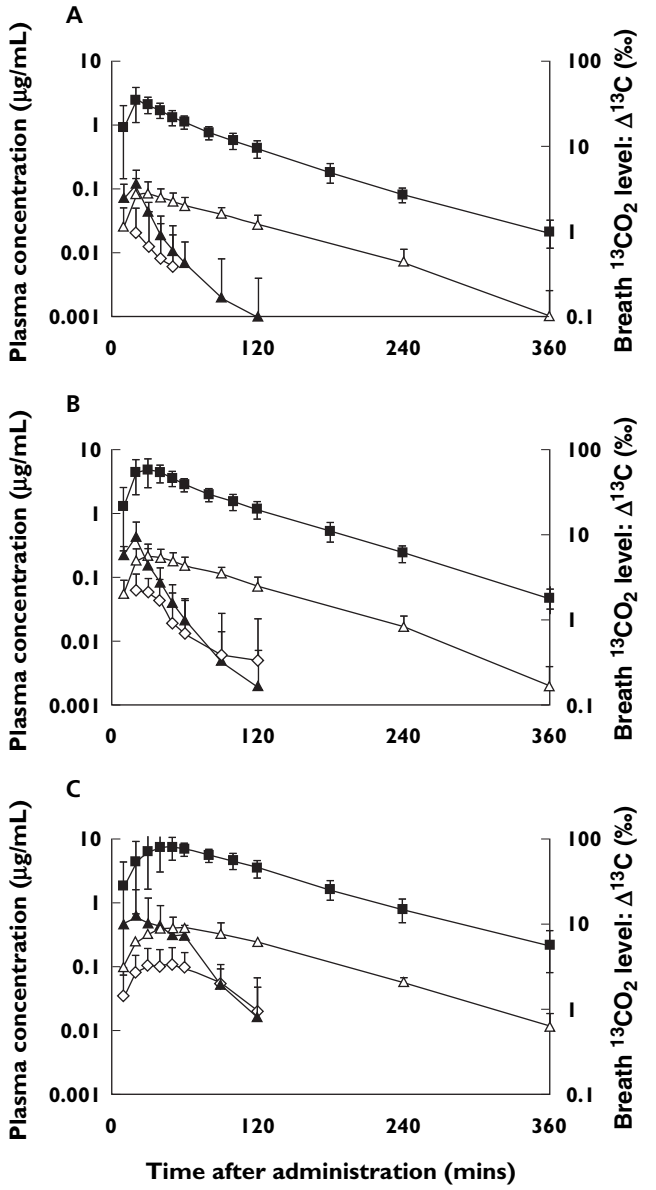

Figure 3

Plasma concentration–time curves for ^{13}C-uracil and its metabolites, and Δ^{13}C–time curves in expired air after oral administration of ^{13}C-uracil at doses of (A) 50 mg, (B) 100 mg, and (C) 200 mg to 12 healthy males. (▲; ^{13}C-uracil, Δ; ^{13}C-DHU, ◇; ^{13}C-UPA, ■; $^{13}CO_2$, mean ± SD, n = 12)

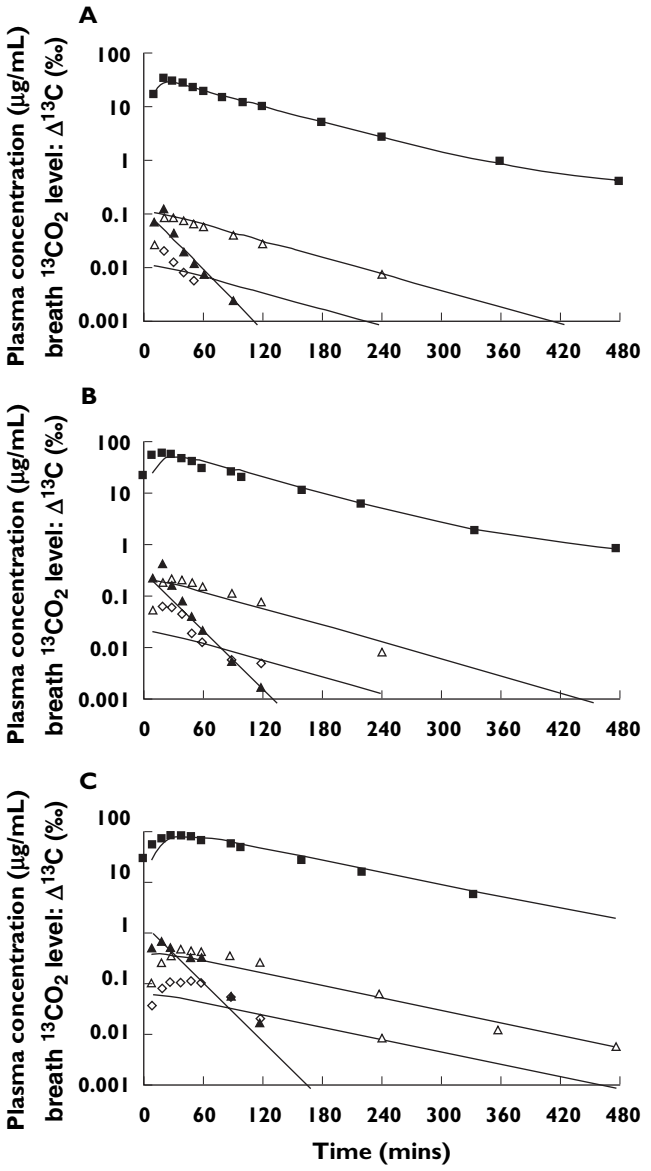

Figure 4

Model fits for the mean plasma concentration–time data for ^{13}C-uracil and its metabolites, and Δ^{13}C in the expired air after oral administration of ^{13}C-uracil at doases of (A) 50 mg, (B) 100 mg, and (C) 200 mg to 12 healthy males. (▲; ^{13}C-uracil, Δ; ^{13}C-DHU, ◇; ^{13}C-UPA, ■; $^{13}CO_2$). Solid lines represent the predicted values calculated by the PBPK model shown in Figure 2

uracil and ^{13}C-DHU (5 ng ml^{-1}), thus introducing some uncertainty into the data. The pharmacokinetic parameters estimated by nonlinear least squares regression are listed in Table 6. The clearance down each metabolic step was calculated as follows: intrinsic clearance (CL_{int1}) for the first step catalysed by DPD was assumed to be V_{max}/K_m, clearance (CL_{int2}) for the second step catalysed by DHPase to be $V_{dDHU} \cdot k_{eDHU}$, and clearance (CL_{int3}) for the third step catalysed by UP to be $V_{dUPA} \cdot k_{eUPA}$. We have assumed that, since ^{13}C-DHU and ^{13}C-UPA are generated sequentially only in the liver, their clearance represents intrinsic hepatic clearance. The rank order of metabolic clearances was $CL_{int3} > CL_{int1} > CL_{int2}$ (Table 6).

Discussion

DPD is reported to be the rate-limiting enzyme in the metabolism of pyrimidine and its analogues under *in*

Table 6
Parameters estimated from simultaneous fitting of mean data for ^{13}C-uracil and its metabolites and $^{13}CO_2$ in expired air

Parameter	Dose 50 mg	100 mg	200 mg
K_m (μg ml^{-1})	–	1.60*	–
V_{max} (μg min^{-1})	–	33900*	–
V_p (l)	–	17.2*	–
k_a (min^{-1})	–	0.259*	–
V_{dDHU} (l)	–	408†	–
V_{dUPA} (l)	–	10.0†	–
k_{eDHU} (min^{-1})	0.0119	0.0126	0.00948
k_{eUPA} (min^{-1})	4.58	5.00	2.54
k_e (min^{-1})	0.151	0.0781	0.0578
P1	0.264	0.627	0.365
P2	0.00904	0.00458	0.00368
CL_{int1} (l min^{-1})‡	–	21.2	–
CL_{int2} (l min^{-1})§	4.86	5.14	3.87
CL_{int3} (l min^{-1})¶	45.8	50.0	25.4

*–, Not calculated. *Calculated using plasma concentrations of ^{13}C-uracil at the doses of 50, 100 and 200 mg by equations 1, 2 and 3. †Calculated using plasma concentrations of ^{13}C-uracil and its metabolites and $^{13}CO_2$ in expired air at the dose of 100 mg by equations 4, 5 and 6. ‡Calculated as V_{max}/K_m. §Calculated as $V_{dDHU}\cdot k_{eDHU}$. ¶Calculated as $V_{dUPA}\cdot k_{eUPA}$.*

vivo conditions [29–32]. However, this view has been disputed by others [2, 10, 33]. Wasternack [33] stated that 'In most papers hitherto published, the first step in degradation has been considered as rate-limiting. However, recent results argue against this concept' and 'Under *in vivo* conditions little information is available because intermediates of degradation are not detectable.' Daher *et al.* [10] reported that 'all steps in the sequential 3-step reactions in pyrimidine metabolism have a potential to be rate-limiting and also it is still unclear which enzyme is rate-limiting'. In the present study, assuming that these discrepancies might be attributable problems in the analysis of pyrimidine and its metabolites in plasma or urine, we re-evaluated the pharmacokinetics of ^{13}C-uracil and its metabolites using the high-resolution methods of LC-MS/MS and IRMS.

The results showed that ^{13}C-uracil was reduced to ^{13}C-DHU by DPD in the first catabolic step, which caused its rapid elimination from plasma. DHPase then mediated the conversion of ^{13}C-DHU to ^{13}C-UPA, but the relatively slow rate of this reaction meant that ^{13}C-DHU remained in plasma for much longer than ^{13}C-uracil. Subsequently, since ^{13}C-UPA was rapidly biotransformed to $H^{13}CO_3^-$ by UP, the Δ^{13}C in the expired air *vs.* time curves were similar to the plasma concentration *vs.* time curves of ^{13}C-DHU.

We developed a PBPK model to describe the pharmacokinetics of uracil. PBPK models have been shown to be useful in quantitative evaluation of the metabolism and transport processes of drugs and endogenous substrates under physiological conditions [34–37]. The derived intrinsic clearances for each metabolic step are consistent with the rapid conversion of uracil to DHU, the slow biotransformation of DHU to UPA, and the rapid conversion of UPA to HCO_3^-.

In contrast, Wasternack [33] suggested that the efflux of dihydropyrimidines from mitochondria into cytosol is rate-limiting owing to the cytosolic location of DPD. Thus, uncertainty remains regarding the rate-limiting step in the disposition of pyrimidines *in vivo*, which may involve factors such as the transportation of ^{13}C-uracil and its metabolites into hepatocytes, the location of the three enzymes responsible for its metabolism, and coenzymes such as NADH, NADPH [38].

Sumi *et al.* [39] reported two cases of dihydropyrimidinuria among 21 200 infants in whom urinary pyrimidine and dihydropyrimidine concentrations were measured, and concluded that a defect in DHPase was a probable risk factor for an adverse response to 5-FU therapy. Hamajima *et al.* [40] subsequently analysed the DHPase gene and demonstrated six types of gene mutation. In addition to these reports, 5-fluoro-5,6-dihydrouracil, the substrate of DHPase and the metabolite of 5-FU, is reported to have antitumour cytotoxic activity [41], suggesting its involvement in the toxicity of 5-FU. Given that the metabolic characteristics of 5-FU [42, 43] and uracil are similar, the present results for uracil should be applicable to 5-FU. Therefore, we came to the tentative hypothesis that the *in vivo* rate-limiting enzyme for 5-FU metabolism is not DPD but DHPase. This hypothesis is supported by a study [9] of [6-^{3}H]5-FU that produced pharmacokinetic profiles of the drug and its metabolites comparable to our results for ^{13}C-uracil. However, in DPD-deficient subjects, DPD is likely to be the rate-limiting enzyme for overall pyrimidine catabolism.

In conclusion, we investigated the metabolic fate of ^{13}C-uracil, its metabolites and the end product $^{13}CO_2$ in expired air. Our PBPK model described the nonlinear pharmacokinetics of uracil and its metabolites well, and showed that of the three enzymes involved in pyrimidine degradation, DHPase is the least active *in vivo* in humans. Further study is required to show whether the analysis of $^{13}CO_2$ in expired air after administration of

^{13}C-uracil will allow the identification of patients at risk of a severe adverse response to treatment with 5-FU.

Competing interests: None declared.

References

1 Sonoda T, Tatibana M. Metabolic fate of pyrimidines and purines in dietary nucleic acids ingested by mice. Biochim Biophys Acta 1978; 521: 55–66.

2 Traut TW, Loechel S. Pyrimidine catabolism: individual characterization of the three sequential enzymes with a new assay. Biochemistry 1984; 23: 2533–9.

3 Canellakis ES. Pyrimidine metabolism. Enzymatic pathway of uracil and thymine degradation. J Biol Chem 1956; 221: 315–31.

4 Fritzson P. Catabolism of C^{14}-labelled uracil, dihydrouracil and β-ureidopropionic acid in rat liver slices. J Biol Chem 1957; 226: 223–8.

5 Diasio RB, Harris BE. Clinical pharmacology of 5-fluorouracil. Clin Pharmacokinet 1989; 16: 215–37.

6 Pinedo HM, Peters GF. Fluorouracil: biochemistry and pharmacology. J Clin Oncol 1988; 6: 1653–64.

7 Ho DH, Townsend L, Luna MA, Bodey GP. Distribution and inhibition of dihydrouracil dehydrogenase activities in human tissues using 5-fluorouracil as a substrate. Anticancer Res 1986; 6: 781–4.

8 Woodcock TM, Martin DS, Damin LA, Kemeny NE, Young CW. Combination clinical trials with thymidine and fluorouracil: a phase I and clinical pharmacologic evaluation. Cancer 1980; 45: 1135–43.

9 Heggie GD, Sommadossi JP, Cross DS, Huster WJ, Diasio RB. Clinical pharmacokinetics of 5-fluorouracil and its metabolites in plasma, urine, and bile. Cancer Res 1987; 47: 2203–6.

10 Daher GC, Harris BE, Diasio RB. Metabolism of pyrimidine analogues and their nucleosides. Pharmacol Ther 1990; 48: 189–222.

11 Lyss AP, Lilenbaum RC, Harris BE, Diasio RB. Severe 5-fluorouracil toxicity in a patient with decreased dihydropyrimidine dehydrogenase activity. Cancer Invest 1993; 11: 239–40.

12 Morrison GB, Bastian A, Dela Rosa T, Diasio RB, Takimoto CH. Dihydropyrimidine dehydrogenase deficiency: a pharmacogenetic defect causing severe adverse reactions to 5-fluorouracil-based chemotherapy. Oncol Nurs Forum 1997; 24: 83–8.

13 Okuda H, Nishiyama T, Ogura K, Nagayama S, Ikeda K, Yamaguchi S, Nakamura Y, Kawaguchi Y, Watabe T. Lethal drug interactions of sorivudine, a new antiviral drug, with oral 5-fluorouracil prodrugs. Drug Metab Dispos 1997; 25: 270–3.

14 Okuda H, Ogura K, Kato A, Takubo H, Watabe T. A possible mechanism of eighteen patient deaths caused by interactions of sorivudine, a new antiviral drug, with oral 5-fluorouracil prodrugs. J Pharmacol Exp Ther 1998; 287: 791–9.

15 Bakkeren JA, De Abre RA, Sengers RC, Gabreels FJ, Maas JM, Renier WO. Elevated urine, blood and cerebrospinal fluid levels of uracil and thymine in a child with dihydrothymine dehydrogenase deficiency. Clin Chim Acta 1984; 140: 247–56.

16 Berger R, Stoker-de Vries SA, Wadman SK, Duran M, Beemer FA, de Bree PK, Weits-Binnerts JJ, Penders TJ, van der Woude JK. Dihydropyrimidine dehydrogenase deficiency leading to thymine-uraciluria. An inborn error of pyrimidine metabolism. Clin Chim Acta 1984; 141: 227–34.

17 Wilcken B, Hammond J, Berger R, Wise G, James C. Dihydropyrimidine dehydrogenase deficiency: a further case. J Inherit Metab Dis 1985; 8: 115–6.

18 Graham DY, Klein PD, Evans DJ Jr, Evans DG, Alpert LC, Opekun AR, Boutton TW. Campylobacter pylori detected noninvasively by the 13C-urea breath test. Lancet 1987; 1: 1174–7.

19 Cutler AF, Havstad S, Ma CK, Blaser MJ, Perez-Perez GI, Schubert TT. Accuracy of invasive and noninvasive tests to diagnose Helicobacter pylori infection. Gastroenterology 1995; 109: 136–41.

20 Goddard AF, Logan RP. Urea breath tests for detecting Helicobacter pylori. Aliment Pharmacol Ther 1997; 11: 641–9.

21 Inada M, Hirao Y, Koga T, Itose M, Kunizaki J, Shimizu T, Sato H. Relationships among plasma [2–^{13}C]uracil concentrations, breath $^{13}CO_2$-expiration, and DPD activity in the liver in normal and DPD-deficient dogs. Drug Metab Dispos 2005; 33: 381–7.

22 Sumi S, Kidouchi K, Kondou M, Hayashi K, Dobashi K, Kouwaki M, Togari H, Wada Y. Possible prediction of adverse reactions to fluorouracil by the measurement of urinary dihydrothymine and thymine. Int J Mol Med 1998; 2: 477–82.

23 Ghoos YF, Maes BD, Geypens BJ, Mys G, Hiele MI, Rutgeerts PJ, Vantrappen G. Measurement of gastric emptying rate of solids by means of a carbon-labeled octanoic acid breath test. Gastroenterology 1993; 104: 1640–7.

24 Meineke I, De Mey C, Eggers R, Bauer FE. Evaluation of the $^{13}CO_2$ kinetics in humans after oral application of sodium bicarbonate as a model for breath testing. Eur J Clin Invest 1993; 23: 91–6.

25 Maes BD, Ghoos YF, Geypens BJ, Mys G, Hiele MI, Rutgeerts PJ, Vantrappen G. Combined carbon-13-glycine/carbon-14-octanoic acid breath test to monitor gastric emptying rates of liquids and solids. J Nucl Med 1994; 35: 824–31.

26 Choi MG, Camilleri M, Burton DD, Zinsmeister AR, Forstrom LA, Nair KS. [^{13}C]octanoic acid breath test for gastric emptying of solids: accuracy, reproducibility, and comparison with scintigraphy. Gastroenterology 1997; 112: 1155–62.

27 Duan LP, Braden B, Caspary WF, Lembcke B. Influence of cisapride on gastric emptying of solids and liquids monitored by ^{13}C breath tests. Dig Dis Sci 1995; 40: 2200–6.

28 Cornetta AM, Simpson KW, Strauss-Ayali D, McDonough PL, Gleed RD. Use of a [^{13}C]urea breath test for detection of gastric infection with Helicobacter spp in dogs. Am J Vet Res 1998; 59: 1364–9.

29 Gonzalez FJ, Fernandez-Salguero P. Diagnostic analysis, clinical importance and molecular basis of dihydropyrimidine dehydrogenase deficiency. Trends Pharmacol Sci 1995; 16: 325–7.

30 Ignoffo RJ. Novel oral fluoropyrimidines in the treatment of metastatic colorectal cancer. Am J Health Syst Pharm 1999; 56: 2417–28.

31 Diasio RB. Clinical implications of dihydropyrimidine dehydrogenase on 5-FU pharmacology. Oncology (Huntingdon) 2001; 15: 21–6.

32 Diasio RB, Johnson MR. The role of pharmacogenetics and pharmacogenomics in cancer chemotherapy with 5-fluorouracil. Pharmacology 2000; 61: 199–203.

33 Wasternack C. Degradation of pyrimidines and pyrimidine analogs—pathways and mutual influences. Pharmacol Ther 1980; 8: 629–51.

34 Charnick SB, Kawai R, Nedelman JR, Lemaire M, Niederberger W, Sato H. Perspectives in pharmacokinetics. Physiologically based pharmacokinetic modeling as a tool for drug development. J Pharmacokinet Biopharm 1995; 23: 217–29.

35 Sato H, Sugiyama Y, Sawada Y, Iga T, Hanano M. Physiologically based pharmacokinetics of radioiodinated human beta-endorphin in rats. An application of the capillary membrane-limited model. Drug Metab Dispos 1987; 15: 540–50.

36 Nagata O, Murata M, Kato H, Terasaki T, Sato H, Tsuji A. Physiological pharmacokinetics of a new muscle-relaxant, inaperisone, combined with its pharmacological effect on blood flow rate. Drug Metab Dispos 1990; 18: 902–10.

37 Sato H, Terasaki T, Mizuguchi H, Okumura K, Tsuji A. Receptor-recycling model of clearance and distribution of insulin in the perfused mouse liver. Diabetologia 1991; 34: 613–21.

38 Smith AE, Yamada EW. Dihydrouracil dehydrogenase of rat liver. Separation of hydrogenase and dehydrogenase activities. J Biol Chem 1971; 246: 3610–7.

39 Sumi S, Imaeda M, Kidouchi K, Ohba S, Hamajima N, Kodama K, Togari H, Wada Y. Population and family studies of dihydropyrimidinuria: prevalence, inheritance mode, and risk of fluorouracil toxicity. Am J Med Genet 1998; 78: 336–40.

40 Hamajima N, Kouwaki M, Vreken P, Matsuda K, Sumi S, Imaeda M, Ohba S, Kidouchi K, Nonaka M, Sasaki M, Tamaki N, Endo Y, De Abreu R, Rotteveel J, van Kuilenburg A, van Gennip A, Togari H, Wada Y. Dihydropyriminase deficiency: structural organization, chromosomal localization, and mutation analysis of the human dihydropyrimidinase gene. Am J Hum Genet 1998; 63: 717–26.

41 Diasio RB, Schuetz JD, Wallace HJ, Sommadossi JP. Dihydrofluorouracil, a fluorouracil catabolite with antitumor activity in murine and human cells. Cancer Res 1985; 45: 4900–3.

42 Collins JM, Dedrick RL, King FG, Speyer JL, Myers CE. Nonlinear pharmacokinetic models for 5-fluorouracil in man: intravenous and intraperitoneal routes. Clin Pharmacol Ther 1980; 28: 235–46.

43 Wagner JG, Gyves JW, Stetson PL, Walker-Andrews SC, Wollner IS, Cochran MK, Ensminger WD. Steady-state nonlinear pharmacokinetics of 5-fluorouracil during hepatic arterial and intravenous infusions in cancer patients. Cancer Res 1986; 46: 1499–506.